Inorg. Chem. **2006**, *45*, 6828–6839

On the Paucity of Molecular Actinide Complexes with Unsupported Metal–Metal Bonds: A Comparative Investigation of the Electronic Structure and Metal–Metal Bonding in U_2X_6 (X = Cl, F, OH, NH_2, CH_3) Complexes and d-Block Analogues

Germán Cavigliasso and Nikolas Kaltsoyannis*

Department of Chemistry, University College London, 20 Gordon Street, London WC1H 0AJ, United Kingdom

Received May 8, 2006

Density functional calculations have been performed on M_2X_6 complexes (where M = U, W, and Mo and X = Cl, F, OH, NH_2, and CH_3) to investigate general aspects of their electronic structures and explore the similarities and differences in metal–metal bonding between f-block and d-block elements. A detailed analysis of the metal–metal interactions has been conducted using molecular orbital theory and energy decomposition methods. Multiple (σ and π) bonding is predicted for all species investigated, with predominant f–f and d–d metal orbital character, respectively, for U and W or Mo complexes. The energy decomposition analysis involves contributions from orbital interactions (mixing of occupied and unoccupied orbitals), electrostatic effects (Coulombic attraction and repulsion), and Pauli repulsion (associated with four-electron two-orbital interactions). The general results suggest that the overall metal–metal interaction is stronger in the Mo and W species, relative to the U analogues, as a consequence of a significantly less destabilizing contribution from the combined Pauli and electrostatic ("pre-relaxation") effects. Although the orbital-mixing ("post-relaxation") contribution to the total bonding energy is predicted to have a larger magnitude in the U complexes, this is not sufficiently strong to compensate for the comparatively greater destabilization that originates from the Pauli-plus-electrostatic effects. Of the pre-relaxation terms, the Pauli repulsion is comparable in analogous U and d-block compounds, contrary to the electrostatic term, which is (much) less favorable in the U systems than in the W and Mo systems. This generally weak electrostatic stabilization accounts for the large pre-relaxation destabilization in the U complexes and, ultimately, for the relative weakness of the U–U bonds. The origin of the small electrostatic term in the U compounds is traced primarily to MX_3 fragment overlap effects.

1. Introduction

The chemistry of transition-element compounds that contain metal−metal bonds is a vast and active field of chemical research.[1] Indeed, metal−metal bonded compounds are known for every member of the d-block, and the study of such metal−metal interactions is interesting and important for several reasons. At a fundamental level, there are the distinct characteristics of bonding between metal atoms, but metal−metal bonded species also have a significant role in a variety of more applied fields, such as metal surfaces, electronic and magnetic devices, catalysis, and bioinorganic chemistry.[2−4]

In contrast to the d-block elements, actinide compounds that contain unsupported metal−metal bonds have been proven to be extremely difficult to synthesize, and known cases are limited to matrix-isolated species, for example, the uranium hydrides with U_2H_2 and U_2H_4 chemical compositions.[5] Indeed, the synthesis of a stable actinide compound with an unsupported metal−metal bond remains somewhat similar to a "Holy Grail" in actinide chemistry. Given this

* To whom correspondence should be addressed. E-mail: n.kaltsoyannis@ucl.ac.uk.

(1) Cotton, F. A.; Walton, R. A. *Multiple Bonds between Metal Atoms*, Second Edition; Oxford University Press: New York, 1993.
(2) Alexeev; O. S.; Gates, B. C. *Ind. Eng. Chem. Res.* **2003**, *42*, 1571.
(3) Adams, R. D., Cotton, F. A., Eds. *Catalysis by Di- and Polynuclear Metal Cluster Complexes*; Wiley−VCH: New York, 1998.
(4) Holm, R. H.; Kennepohl, P.; Solomon, E. I. *Chem. Rev.* **1996**, *96*, 2239.
(5) Souter, P. F.; Kushto, G. P.; Andrews, L.; Neurock, M. *J. Am. Chem. Soc.* **1997**, *119*, 1682.

10.1021/ic060777e CCC: $33.50
Published on Web 07/26/2006

Chart 1

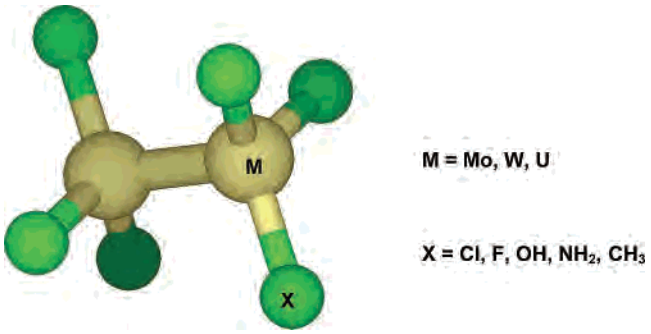

paucity, computational chemistry is a particularly valuable tool in the investigation and understanding of metal−metal bonding involving 5f elements. A number of studies have been conducted at various levels of theory and include investigations both of simple molecules such as U_2,[6,7] Pu_2,[8] and Th_2H_2,[9] as well as some dinuclear uranium complexes.[5,10−12] The most recent multiconfigurational wave function calculations, by Roos and Gagliardi, on various dinuclear uranium−chloride and uranium−carboxylate complexes have predicted that these species should be stable and contain a multiply bonded U_2 unit.[12]

In this article, we report the results of density functional calculations on a series of model uranium, tungsten, and molybdenum M_2X_6 (X = Cl, F, OH, NH_2, CH_3) species (Chart 1). The metal atoms in these complexes have a formal oxidation state of +3, leading to metal-based electronic configurations that can be formally described as d^3d^3 for the Mo and W species, and f^3f^3 for the U systems. A metal−metal triple bond is, in principle, possible in all cases, but it might be anticipated that the details of the metal−metal interactions between d-block and f-block elements should be different. In the present work, we have performed an extensive molecular orbital and energy decomposition analysis, to gain detailed insight into the nature of the electronic structures and the similarities and differences in metal−metal interactions between the d-block and f-block elements. In particular, we are keen to establish if there are intrinsic intramolecular reasons why metal−metal bonding in the actinides is so rare.

2. Computational Details

All density functional calculations reported in this article were performed with the Amsterdam Density Functional (ADF 2004) program.[13−15] A Generalized-Gradient-Approximation (GGA) functional, which consisted of the exchange expression proposed by Handy and Cohen[16] and the correlation expression proposed by Perdew, Burke, and Ernzerhof[17] (labeled OPBE), was utilized. Basis sets of triple-ζ quality and one polarization function (TZP or type IV), incorporating frozen cores (C.1s, N.1s, O.1s, F.1s, Cl.2p, Mo.3d, W.4f, U.5d), were used.[13−15] This choice of frozen cores implies that the "outer core plus valence" (Mo [4s4p4d5s5p], W [5s5p5d6s6p], U [6s6p6d7s7p5f]) regions of the metal atom basis sets are comparable or equivalent in character and size. Relativistic effects were included by means of the Zero Order Regular Approximation (ZORA).[18−20] Plots of the molecular orbitals were generated with the MOLEKEL program,[21,22] using data in MOLDEN format[23,24] that was derived from the ADF TAPE21 files.

The choice of functional was based on a series of tests performed on M_2X_6 complexes (M = Mo, W; X = NH_2, CH_3) and a comparison of the optimized metal−metal distances with experimental observations for Mo−Mo and W−W bond lengths in dinuclear Mo and W species that contain C and N donor ligands. Details of these test calculations are provided as Supporting Information (Tables S1 and S2).

3. Results and Discussion

Experimental investigations of Mo_2X_6 and W_2X_6 complexes that contain a variety of ligands have indicated that these species prefer to adopt a staggered conformation.[1] Recent quantum chemical calculations on U_2Cl_6[12] have also predicted that the staggered form should be more stable than the eclipsed form, by ∼12 kcal/mol (50 kJ/mol). Therefore, all results presented in this article correspond to calculations performed, utilizing ideal D_{3d} molecular symmetry, exclusively on the staggered forms of the Mo, W, and U species studied (see Chart 1).

Calculated structural parameters for all M_2X_6 complexes investigated are presented in Table 1. The computational values for metal−metal distances and metal−metal-ligand angles in the Mo and W complexes are in good agreement with the crystallographic data for M_2X_6 species that contain C, N, and O donor ligands,[1,25] whereas the predicted U−U bond lengths are somewhat shorter than those obtained on related dinuclear uranium systems using multiconfigurational quantum chemical procedures.[12] It is also interesting to mention that the calculated values of all Mo−Mo, W−W,

(6) Pepper, M.; Bursten, B. E. *J. Am. Chem. Soc.* **1990**, *112*, 7803.
(7) Gagliardi, L.; Roos, B. O. *Nature* **2005**, *433*, 848.
(8) Archibong, E. F.; Ray, A. K. *Phys. Rev. A* **1999**, *60*, 5105.
(9) Straka, M.; Pyykkö, P. *J. Am. Chem. Soc.* **2005**, *127*, 13090.
(10) Bursten, B. E.; Schneider, W. F. Theoretical Studies of Dinuclear Compounds with Multiple Metal−Metal Bonds. In *Metal−Metal Bonds and Clusters in Chemistry and Catalysis*; Fackler, J. P., Jr., Ed.; Plenum Press: New York, 1990.
(11) Cayton, R. H.; Novo-Gradac, K. J.; Bursten, B. E. *Inorg. Chem.* **1991**, *30*, 2265.
(12) Roos, B. O.; Gagliardi, L. *Inorg. Chem.* **2006**, *45*, 803.
(13) Amsterdam Density Functional (ADF) Package, Scientific Computing and Modelling NV (SCM), Theoretical Chemistry, Vrije Universiteit, Amsterdam, The Netherlands. Available via the Internet at http://www.scm.com.
(14) Fonseca Guerra, C.; Snijders, J. G.; te Velde, G.; Baerends, E. J. *Theor. Chem. Acc.* **1998**, *99*, 391.
(15) te Velde, G.; Bickelhaupt, F. M.; van Gisbergen, S. J. A.; Fonseca Guerra, C.; Baerends, E. J.; Snijders, J. G.; Ziegler, T. *J. Comput. Chem.* **2001**, *22*, 931.
(16) Handy, N. C.; Cohen, A. *J. Mol. Phys.* **2001**, *99*, 403.
(17) Perdew, J. P.; Burke, K.; Ernzerhof, M. *Phys. Rev. Lett.* **1996**, *77*, 3865.
(18) van Lenthe, E.; Baerends, E. J.; Snijders, J. G. *J. Chem. Phys.* **1993**, *99*, 4597.
(19) van Lenthe, E.; Baerends, E. J.; Snijders, J. G. *J. Chem. Phys.* **1994**, *101*, 9783.
(20) van Lenthe, E.; Ehlers, A. E.; Baerends, E. J. *J. Chem. Phys.* **1999**, *110*, 8943.
(21) MOLEKEL: An Interactive Molecular Graphics Tool. Available via the Internet at http://www.cscs.ch/molekel/.
(22) Portmann, S.; Lüthi, H. P. *Chimia* **2000**, *54*, 766.
(23) MOLDEN: A Pre and Post-processing Program for Molecular and Electronic Structures. Available via the Internet at http://www.cmbi.ru.nl/molden/molden.html.
(24) Schaftenaar, G.; Noordik, J. H. *J. Comput.-Aided Mol. Des.* **2000**, *14*, 123.
(25) Liu, X.-Y.; Alvarez, S. *Inorg. Chem.* **1997**, *36*, 1055.

Table 1. Optimized Structural Parameters of M_2X_6 Complexes

metal	ligand	Distance (pm) M−M	Distance (pm) M−X	bond angle, M−M−X (degrees)
Mo	Cl	223	224	103
Mo	F	225	186	101
Mo	OH	222	192	100
Mo	NH_2	222	202	99
Mo	CH_3	221	210	102
W	Cl	230	225	103
W	F	231	188	102
W	OH	230	193	100
W	NH_2	229	202	99
W	CH_3	229	210	103
U	Cl	235	246	119
U	F	238	204	123
U	OH	237	208	122
U	NH_2	235	218	116
U	CH_3	236	234	124

and U−U distances are similar to the results derived from the triple-bond covalent radii recently proposed by Pyykkö, Riedel, and Patzschke.[26]

Multiconfigurational calculations have also been used to estimate the dissociation energy of U_2Cl_6 into two UCl_3 fragments, which are characterized by a pyramidal structure and a quartet spin state, with the predicted result being ∼20 kcal/mol (84 kJ/mol).[12] Our density functional calculations indicate that the dissociation energy is somewhat smaller (3.05 kcal/mol or 12.76 kJ/mol), but additional tests have revealed that this value is quite sensitive to the type of functional used in the calculations.

3.1. Molecular Orbital Analysis. An integrated approach, involving the decomposition of the M_2X_6 complexes into two MX_3 units possessing ideal C_{3v} symmetry and incorporating the interactions between the MX_3 fragment orbitals and the atomic orbital contributions to the composition of the MX_3 and M_2X_6 orbitals, has been used to perform a molecular orbital analysis of the electronic structure of all species investigated. The results are summarized in Figures 1 and 2.

Valence orbital energy levels are plotted in Figure 1 and a qualitative description of the general orbital compositions and character is presented in Figure 2. Note that only the lowest-lying unoccupied levels are included in these diagrams, and that the valence orbitals whose compositions contain large contributions from Cl, F, O, N, or C s-type functions have also been excluded, because they reside at considerably lower energy than any other group of occupied valence orbitals and are not involved in metal−ligand interactions.

A common feature of the molecular orbital structure of all Mo, W, and U species investigated, as represented in Figure 2, is the presence of three distinct sets of levels. The orbitals that comprise the lowest-lying set are primarily associated with the ligands, and their compositions exhibit large contributions from Cl, F, O, N, or C *p*-type functions. These orbitals are either nonbonding (that is, strictly or almost completely ligand-based) or metal−ligand bonding. In the latter case, the orbital compositions show greater metal contributions in the Mo and W species, compared with the U systems. For example, the contributions from Mo or W orbitals can be as high as 30%−40%, whereas those from U orbitals are typically <20%. These results thus suggest that the metal−ligand bonds formed by the d-block elements are characterized by greater covalent character.

Generally, for the Mo and W complexes, the metal orbitals involved in the bonding to the ligands are predominantly of d character, with minor participation of s and p orbitals (especially the latter). However, a difference between Mo and W species is observed in that the W s-type functions seem to make relatively important contributions to some metal−ligand bonding orbitals (for example, the W s-type contributions to the $5a_{1g}$ orbital of $W_2(CH_3)_6$ is 25%), although their overall participation is rather small, relative to the W d-type functions. In the case of the U complexes, both d and f orbitals have a role in the metal−ligand bonding interactions, with the former having somewhat greater contributions, whereas no significant involvement of s or p orbitals is observed.

The orbitals primarily associated with metal−metal bonding are the $6a_{1g}$ and $6e_u$ levels. Their compositions are given in Table 2, in terms of metal and ligand contributions, and are also represented schematically, using interaction diagrams involving fragment and atomic orbitals, in Figure 2. As shown by the three-dimensional representations included in this figure, the $6a_{1g}$ and $6e_u$ orbitals possess metal−metal σ and π bonding character, respectively. The e_g and e_u irreducible representations in D_{3d} symmetry encompass metal−metal interactions between d or f orbitals of both π and δ character. However, as revealed by the plots given in Figure 2, the $6e_u$ orbitals are predominantly π-like, because the δ-type interactions represent only minor contributions to their composition.

For the Mo and W complexes, the $6a_{1g}$ and $6e_u$ orbitals arise primarily from interactions between the (highest occupied) $6a_1$ and 6e orbitals in the MX_3 fragments (Table 3). In addition, in some of the species studied, the $5a_1$, 5e, and 7e fragment orbitals are also involved, albeit to a much smaller degree, in the composition of the metal−metal bonding orbitals.

Table 2 indicates that the Mo−Mo and W−W σ and π bonds are predominantly of d character, with considerably smaller participation of s-type functions and only minimal contributions from *p*-type functions. Nevertheless, metal−metal σ bonding does exhibit some s character, which is, generally, somewhat more significant for the W complexes than for the Mo complexes (a result also observed in previous comparative investigations of Mo and W species, using relativistic density functional approaches [27,28]). Significant ligand contributions to the $6e_u$ orbitals are observed, with the exception of $Mo_2(CH_3)_6$ and $W_2(CH_3)_6$, and the three-dimensional representations in Figure 2 show that the resulting metal−ligand interaction has d(M)−p(L) π-antibonding properties. Generally, considerably smaller ligand contributions to the $6a_{1g}$ orbital are observed, and, therefore, this orbital is largely metal−metal-based.

(26) Pyykkö, P.; Riedel, S.; Patzschke, M. *Chem. Eur.*−*J.* **2005**, *11*, 3511.

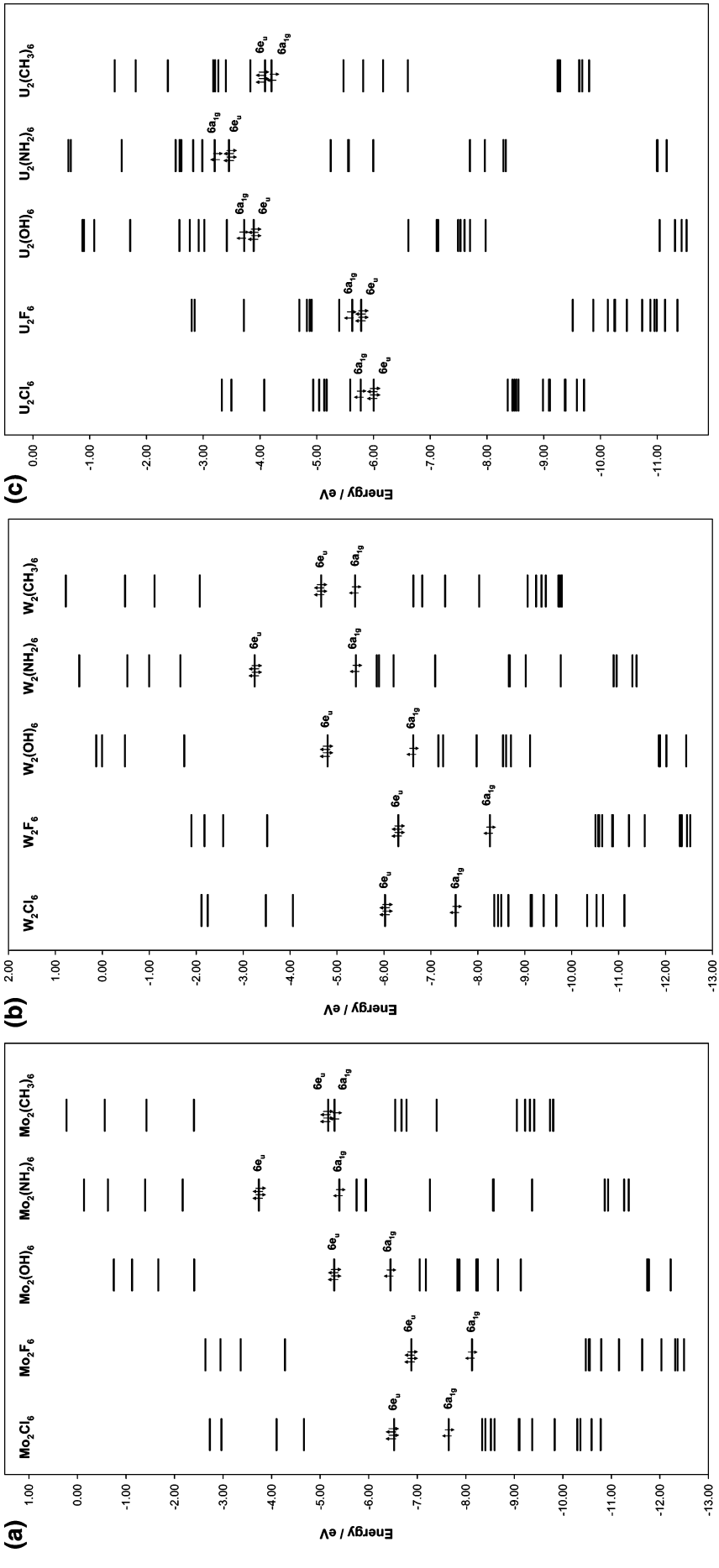

Figure 1. Orbital energy levels (valence shell) for M_2X_6 complexes where M = (a) Mo, (b) W, and (c) U. The small arrows are used to identify the levels associated with the metal−metal triple bond, which are the highest occupied orbitals in all cases.

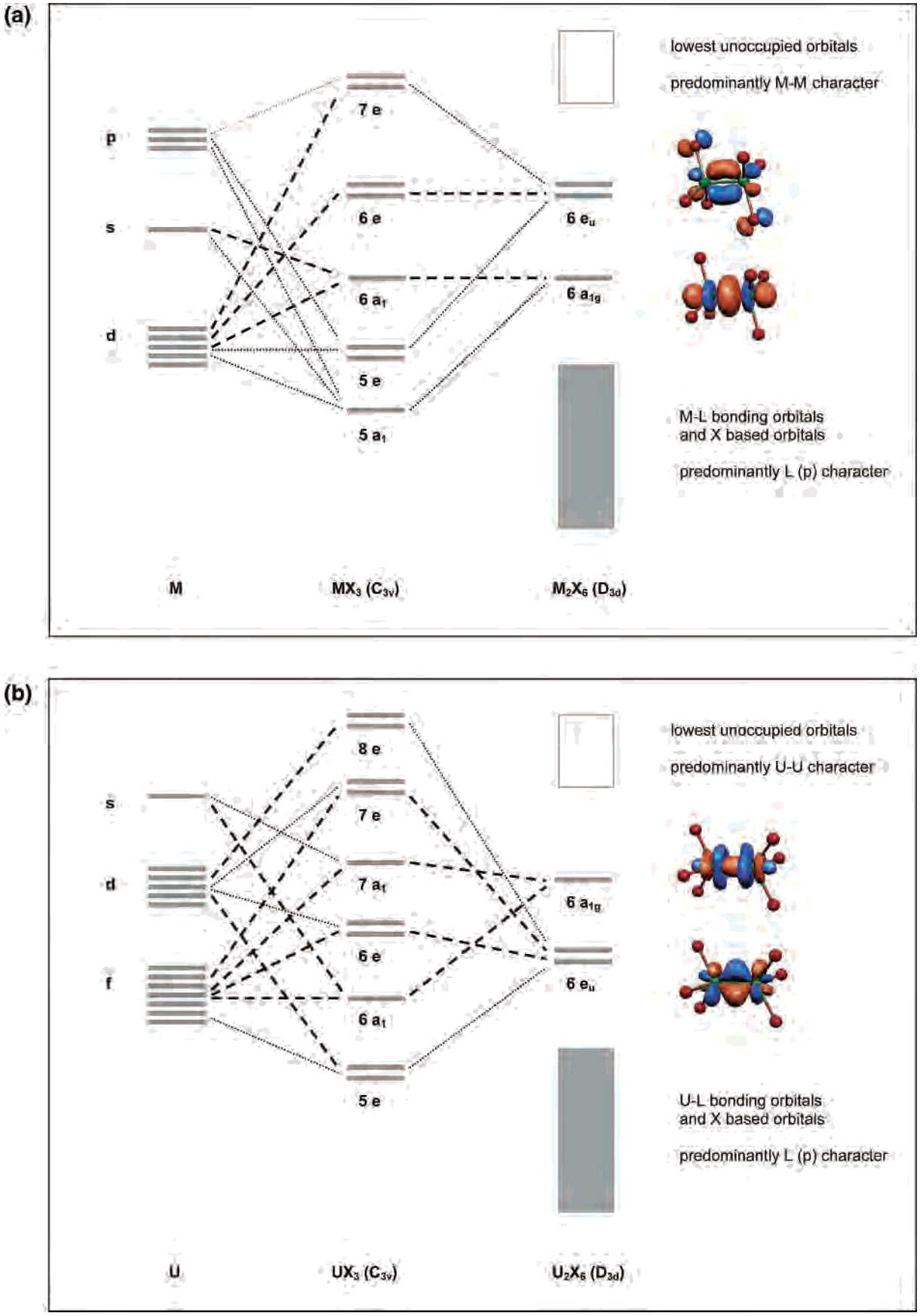

Figure 2. General qualitative representation of the molecular orbital structure (valence shell) of M_2X_6 complexes (L = Cl, F, N, O, C; X = Cl, F, OH, NH_2, CH_3) and composition of the metal−metal bonding orbitals ((a) Mo and W, and (b) U). Major and minor contributions are indicated by dashed and dotted lines, respectively.

Table 2. Composition of Metal−Metal Bonding Orbitals of M_2X_6 Complexes

		Composition (%)								
		$6a_{1g}$ (σ) orbital					$6e_u$ (π) orbital			
metal	ligand	f^a	d^a	s^a	p^a	L^b	f^a	d^a	p^a	L^b
Mo	Cl		69	8	3	13		46	2	48
Mo	F		70	11	2	8		64	2	29
Mo	OH		74	14		4		63	2	27
Mo	NH_2		72	14		8		49		38
Mo	CH_3		73	11		7		80	5	3
W	Cl		68	15	3	10		54	4	40
W	F		65	24	3	4		69	4	26
W	OH		70	23		4		70	3	21
W	NH_2		58	14	2	21		54		37
W	CH_3		81	12		1		81	5	2
U	Cl	76	2	12	3	3	73	13	1	10
U	F	69	2	20	6	2	75	15	1	6
U	OH	66	2	22	5	2	78	13	1	3
U	NH_2	70	1	19	2	6	70	21	1	4
U	CH_3	66	6	18	6		79	10	1	8

[a] The *f*, *d*, *s*, and *p* labels describe contributions from the corresponding metal orbitals. [b] The *L* label represents contributions from Cl, F, O, N, or C orbitals.

Table 3. Composition of Metal-Based Orbitals of MoX_3 and WX_3 Fragments

		Composition (%)					
		6 a_1 orbital				6 e orbital	
metal	ligand	d^a	s^a	p^a	L^b	d^a	L^b
Mo	Cl	77	12	1	7	75	20
Mo	F	71	21	1	5	82	14
Mo	OH	70	26	2		82	12
Mo	NH_2	69	27		3	79	12
Mo	CH_3	70	20	1	5	89	
W	Cl	71	22	1	4	78	20
W	F	61	39	2	2	85	11
W	OH	62	36		2	85	11
W	NH_2	63	34	2		81	12
W	CH_3	70	26	2		89	

[a] The *d*, *s*, and *p* labels describe contributions from the corresponding metal orbitals. [b] The *L* label represents contributions from Cl, F, O, N, or C orbitals.

Table 4. Composition of Metal-Based Orbitals of UX_3 Fragments

	Composition (%)															
	6 a_1 orbital				7 a_1 orbital			6 e orbital			7 e orbital			
ligand	f^a	s^a	p^a	L^b	f^a	s^a	d^a	f^a	d^a	L^b	f^a	p^a	d^a	L^b
Cl	82	14		1	98			95	3	1	90	1	6	2
F	63	38	2		96	4		90	9		85		12	1
OH	64	37	1		96	3		92	6		83		14	2
NH_2	60	39	2		98			92	7		84		12	3
CH_3	71	27	2		95	3	2	94	3		86		13	

[a] The *f*, *s*, *p*, and *d* labels describe contributions from the corresponding metal orbitals. [b] The *L* label represents contributions from Cl, F, O, N, or C orbitals.

The metal−metal σ and π bonds in the U complexes are the result of interactions that involve both occupied and virtual fragment orbitals, with the (UX_3) $6a_1$ and $7a_1$ orbitals and 6e and 7e orbitals being the major contributions to the (U_2X_6) $6a_{1g}$ and $6e_u$ orbitals, respectively (Table 4). For U_2Cl_6 and $U_2(CH_3)_6$, there is also minor participation of the 8e and 5e fragment orbitals, respectively, in the U−U π interactions. The $6a_{1g}$ and $6e_u$ orbitals of all U_2X_6 complexes contain only minor ligand contributions, and, thus, are largely U−U based with predominant f character (as shown by the plots in Figure 2b). Nevertheless, some participation of s-type and d-type functions in the σ and π bonding interactions is also predicted (see Table 2).

The highest-lying set of molecular energy levels in the schematic diagrams of Figure 2 contains the lowest unoccupied orbitals, which possess mostly metal−metal character in all Mo, W, and U complexes investigated, although significant ligand character in some Mo and W species is also observed. These orbitals correspond to metal−metal δ bonding and antibonding and σ and π antibonding interactions in the case of the Mo and W complexes, and metal−metal δ and ϕ bonding and antibonding and σ and π antibonding interactions in the case of the U species.

Examination of the energy-level diagrams in Figure 1 reveals some additional similarities and differences in the electronic structures of the Mo, W, and U complexes. Generally, a clear separation is predicted between the highest-occupied $6a_{1g}$ and $6e_u$ orbitals and the predominantly ligand-based set of orbitals that reside at lower energy, with the gap between these two distinct groups of levels being greater for the U species than for the Mo and W analogues.

The $6a_{1g}$ (metal−metal σ-bonding) orbitals occur at a (significantly) lower energy than the $6e_u$ (metal−metal π-bonding) orbitals for the Mo and W complexes, whereas the opposite ordering (except for $U_2(CH_3)_6$) and (much) smaller energy gaps are observed in the U analogues. This predicted destabilization of the $6e_u$ orbitals, with respect to the $6a_{1g}$ orbitals, in the Mo and W species correlates with the fact that the former possess some significant metal−ligand antibonding character, in addition to their predominant metal−metal bonding character (see Figure 2).

The separation between the highest occupied molecular orbitals (HOMOs) and lowest unoccupied molecular orbitals (LUMOs) is considerably smaller for the U systems than for the Mo and W species, and the HOMO−LUMO gaps in the U complexes are actually sufficiently small to suggest that triplet, quintet, and septet states that result from the decoupling, and promotion to higher levels, of the $6a_{1g}$ and $6e_u$ electrons may be of comparable energy to the metal−metal multiply bonded singlet state. We have confirmed this general observation through several additional calculations, using different density functionals. However, we are primarily interested in a direct comparison of metal−metal bonding in d-block and f-block species and, therefore, we have focused exclusively on the U_2X_6 singlet state. It is also worth noting that the multiconfigurational calculations on U_2Cl_6 recently reported by Roos and Gagliardi favor the singlet state,[12] although a triplet state, lying only 2 kcal/mol (8.4 kJ/mol) to higher energy, is also predicted.

Bursten and Schneider have studied the electronic structure of $U_2(CH_3)_6$,[10] at a lower level of theory than the present density functional calculations, and an interesting finding of

(27) Bridgeman, A. J.; Cavigliasso, G. *J. Chem. Soc., Dalton Trans.* **2001**, 3556.

(28) Bridgeman, A. J.; Cavigliasso, G. *J. Phys. Chem. A* **2003**, *107*, 4568.

Table 5. Energy Decomposition Analysis of M_2X_6 Complexes[a]

		Energy Decomposition Result (eV)							
metal	ligand	E_B	$E_P + E_E$	E_P	E_E	E_O	E_O (a_1)	E_O (e)	E_O (a_2)
Mo	Cl	−3.24	4.73	12.51	−7.78	−7.97	−3.30	−4.67	0.00
Mo	F	−3.23	4.38	12.81	−8.43	−7.62	−3.31	−4.31	0.00
Mo	OH	−3.19	4.64	12.80	−8.16	−7.83	−3.23	−4.61	0.00
Mo	NH_2	−2.56	4.41	14.43	−10.02	−6.98	−3.18	−3.79	0.00
Mo	CH_3	−3.28	4.50	16.34	−11.83	−7.78	−2.96	−4.82	0.00
W	Cl	−4.34	4.02	15.45	−11.42	−8.37	−3.37	−5.00	0.00
W	F	−4.46	3.67	15.35	−11.68	−8.12	−3.29	−4.83	0.00
W	OH	−4.19	3.93	14.53	−10.60	−8.12	−3.22	−4.90	0.00
W	NH_2	−3.46	4.00	17.00	−13.00	−7.46	−3.27	−4.19	0.00
W	CH_3	−4.08	3.83	18.52	−14.70	−7.91	−3.04	−4.87	0.00
U	Cl	−0.20	10.44	11.39	−0.95	−10.64	−3.56	−6.98	−0.10
U	F	−1.22	9.86	12.67	−2.80	−11.08	−4.53	−6.50	−0.05
U	OH	−1.00	9.39	16.76	−7.37	−10.39	−3.77	−6.57	−0.04
U	NH_2	−1.09	9.47	14.13	−4.66	−10.55	−3.71	−6.83	0.00
U	CH_3	−1.39	10.32	19.56	−9.24	−11.72	−4.39	−7.32	0.00

[a] Results correspond to eq 3. Legend for table is as follows: E_B, total bonding energy; E_P, Pauli repulsion, E_E, electrostatic interaction; and E_O, orbital mixing.

their investigation is that significant overlap between the U−C and U−U energy levels is predicted, which leads to a direct competition between the U−C σ and U−U δ interactions, which should be favorable for metal−metal bond formation but detrimental to the overall stability of the system. These results are not reproduced by our calculations, which indicate that a significant energy gap (∼1.2−1.3 eV) separates the primary metal−metal bonding levels ($6a_{1g}$ and $6e_u$) from the metal−ligand levels and that, even though U−U δ bonds are observed in the triplet, quintet, and septet spin states, the electrons involved in these δ-type interactions are taken from the U−U σ ($6a_{1g}$) and π ($6e_u$) orbitals, rather than from the metal−ligand orbitals.

3.2. Energy Decomposition Analysis. An analysis of bonding energetics can be performed by combining a fragment approach to the molecular structure of a chemical system with the decomposition of the total bonding energy (E_B), as

$$E_B = E_E + E_P + E_O \quad (1)$$

where E_E, E_P, and E_O are, respectively, electrostatic interaction, Pauli repulsion, and orbital mixing terms. A detailed description of the physical significance of these properties has been given by Bickelhaupt and Baerends.[29]

The bonding energy (E_B) can be considered a measure of the "instantaneous" interactions between the fragments in the molecule, but it does not represent the bond dissociation energy (E_D), which is defined as

$$E_D = E_B + E_F \quad (2)$$

and contains, in addition to the bonding energy, a contribution arising from the fragment preparation processes (E_F), which can be described as the energy associated with the fragments' transformation from their equilibrium geometry and electronic state into their "intrinsic" geometric and electronic states in the molecule.

The electrostatic component is calculated from the superposition of the unperturbed fragment densities at the molecular geometry and corresponds to the classical electrostatic effects associated with Coulombic attraction and repulsion. The electrostatic contribution is most commonly dominated by the nucleus−electron attractions and, therefore, has a stabilizing influence. The Pauli component is obtained by requiring that the electronic antisymmetry conditions be satisfied, and has a destabilizing character, whereas the orbital mixing component represents a stabilizing factor that originates from the relaxation of the molecular system, due to the mixing of occupied and unoccupied orbitals, and can involve electron-pair bonding, charge-transfer or donor−acceptor interactions, and polarization.

3.2.1. General Bonding Energy Results. The fragments used in the energy decomposition analysis can take any chemical form, including single atoms and ions, as well as (electrically) neutral or charged molecular units. In addition, several electronic states may be possible and plausible for the separated fragments.

In the present work, the fragment chemical and electronic structures have been chosen so that they correspond, as closely as possible, to the [$\sigma + 2\pi$] multiple bonding environment in the (D_{3d}) M_2X_6 molecular system. Thus, the most natural "fragmentation" scheme for the analysis of the metal−metal interactions in these complexes is

$$[X_3M]\ (\uparrow\uparrow\uparrow) + (\downarrow\downarrow\downarrow)\ [MX_3] \leftrightarrow M_2X_6 \quad (3)$$

where the MX_3 fragments possess ideal C_{3v} symmetry and have three unpaired electrons (represented by the arrows) associated with a $[(6a_1)^1(6e)^2]$ orbital occupation (see Figure 2).

The results that correspond to the fragment and energy decomposition analyses of all M_2X_6 complexes studied in the present work are summarized in Table 5. In addition to the individual components in eq 1, values for a combined "Pauli plus electrostatic" ($E_P + E_E$) contribution and a decomposition of the orbital-mixing term using C_{3v} irreducible representations are included. The combined Pauli−

(29) Bickelhaupt, F. M.; Baerends, E. J. *Rev. Comput. Chem.* **2000**, *15*, 1.

electrostatic and the orbital-mixing contributions respectively represent measures of the fragment interaction before and after electronic relaxation through a self-consistent-field procedure has occurred, and can thus be described as "pre-relaxation" and "post-relaxation" effects.

The total bonding energy results suggest that the metal−metal interactions are significantly stronger in the Mo and W complexes than in the U analogues, because of a considerably more destabilizing influence of the pre-relaxation ($E_P + E_E$) contributions in the latter. In contrast, the orbital-mixing component is actually larger in magnitude in the U species, but the difference with respect to the Mo and W systems is not sufficiently large to compensate for the stronger destabilization that originates from the pre-relaxation effects.

Further analysis of the pre-relaxation terms shows that the Pauli repulsion is larger in magnitude than the electrostatic component and is ultimately responsible for the overall destabilizing character of the pre-relaxation fragment interactions. However, although the effects of Pauli repulsion across the Mo, W, and U series are comparable, the electrostatic interaction is (markedly) weaker in the U species, and this is the primary reason for the overall lower strength of the U−U bonds, relative to the Mo−Mo and W−W bonds.

The optimized metal−metal distances of the U complexes are longer than those of the Mo and W analogues, and it is therefore necessary to assess whether this result may be a significant factor in the predicted trends for the bonding energy terms. Thus, we have conducted an extended energy decomposition analysis by means of a potential energy scan in which only the metal−metal separation was varied while the metal−ligand structural parameters were kept fixed at their optimized values. The results for M_2Cl_6 and $M_2(CH_3)_6$ complexes, which represent two "extreme" cases (on the basis of the considerable differences in the respective values for the Pauli and electrostatic components), are shown in Figure 3 and Table 6. (Complete results for all species are given as Supporting Information.)

Table 6 provides a comparison of the bonding energy results for a fixed metal−metal distance of 230 pm, which is somewhat shorter and longer, respectively, than the U−U and Mo−Mo equilibrium bond lengths, and represents approximately the optimized value for the W species. The electrostatic interaction remains much weaker in U_2Cl_6, relative to Mo_2Cl_6 and W_2Cl_6, and, generally, this observation is valid at all metal−metal distances in the vicinity of the minima in the potential energy curves (Figure 3). For $U_2(CH_3)_6$, shortening the U−U bond causes the magnitude of the electrostatic term to become more similar to that of $W_2(CH_3)_6$, and actually somewhat greater than that of $Mo_2(CH_3)_6$, but analogously to U_2Cl_6, its stabilizing contribution is not sufficiently large so as to counteract the Pauli repulsion effects. The results and conclusions from this analysis are also applicable to the remaining M_2X_6 complexes studied, because the behavior of the M_2F_6 and $M_2(NH_2)_6$ species resembles the M_2Cl_6 case, whereas the behavior of the $M_2(OH)_6$ species is similar to the $M_2(CH_3)_6$ case. Overall, the conclusions that concern the factors determining the total bonding energy are not affected by relatively small changes in the metal−metal distance values in the vicinity of the potential energy minima.

Equilibrium bond lengths are determined by the competition between the destabilizing Pauli repulsion and the stabilizing contributions of orbital mixing and electrostatic interactions. An analysis of the rate of change of these properties, within the bond-length range that contains all optimized energy minima (∼220−240 pm), reveals why the metal−metal distances are shortest and longest for Mo and U complexes, respectively, whereas the W−W distances exhibit intermediate values. As the metal−metal bond contracts, the magnitude of the combined orbital mixing and electrostatic terms in the Mo species increases at a somewhat higher rate than does the Pauli repulsion, whereas the opposite result is observed for the U species. For the W complexes, the rates of change of these two factors are more similar to each other, compared to the Mo and U analogues, and the W−W bond lengths are, therefore, not as short or long, respectively, as the Mo−Mo and U−U distances. The Pauli repulsion arises from four-electron two-orbital interactions, and it is possible that the larger radial extension of the outer core ($n - 1$) p atomic orbitals of U, relative to W and Mo, is responsible for the steeper gradient of the Pauli term in the U complexes.

Further insight into the role of the outer-core orbitals in the Pauli repulsion can be gained by performing an energy decomposition analysis using frozen cores that include the ($n - 1$) s and ($n - 1$) p orbitals. A comparison of the results of calculations on the Mo and U complexes, which use both "large-core" (Mo.4p and U.6p) and "small-core" (Mo.3d and U.5d) basis sets, is presented in Table 7. Analogous calculations on the W complexes could not be performed, because of the unavailability of the equivalent large-core basis sets for this element.

Table 7 reveals that the incorporation of the ($n - 1$) s and ($n - 1$) p atomic orbitals into the frozen core has a markedly different effect on the U complexes, compared with the Mo species. In the latter case, only minor changes are observed in each of the energy terms, and, therefore, the primary source of the Pauli repulsion seems to lie in the interactions between the valence MoX_3 orbitals. For the U systems, although the changes that affect the electrostatic and orbital-mixing terms are relatively small, a rather large decrease in the magnitude of the Pauli repulsion is observed. Contrary to the Mo systems, this result suggests that there are significant destabilizing contributions arising from the interactions involving the U outer-core orbitals. Given the general similarities between Mo and W species, it is reasonable to expect that the behavior of the W complexes should resemble that of the Mo systems, rather than the U systems.

3.2.2. Pre-relaxation: Pauli Repulsion and Electrostatic Interactions. Previous investigations of chemical bonding in main-group systems, using the energy decomposition analysis, have shown that trends in Pauli repulsion may be rationalized by considering correlations with occupied frag-

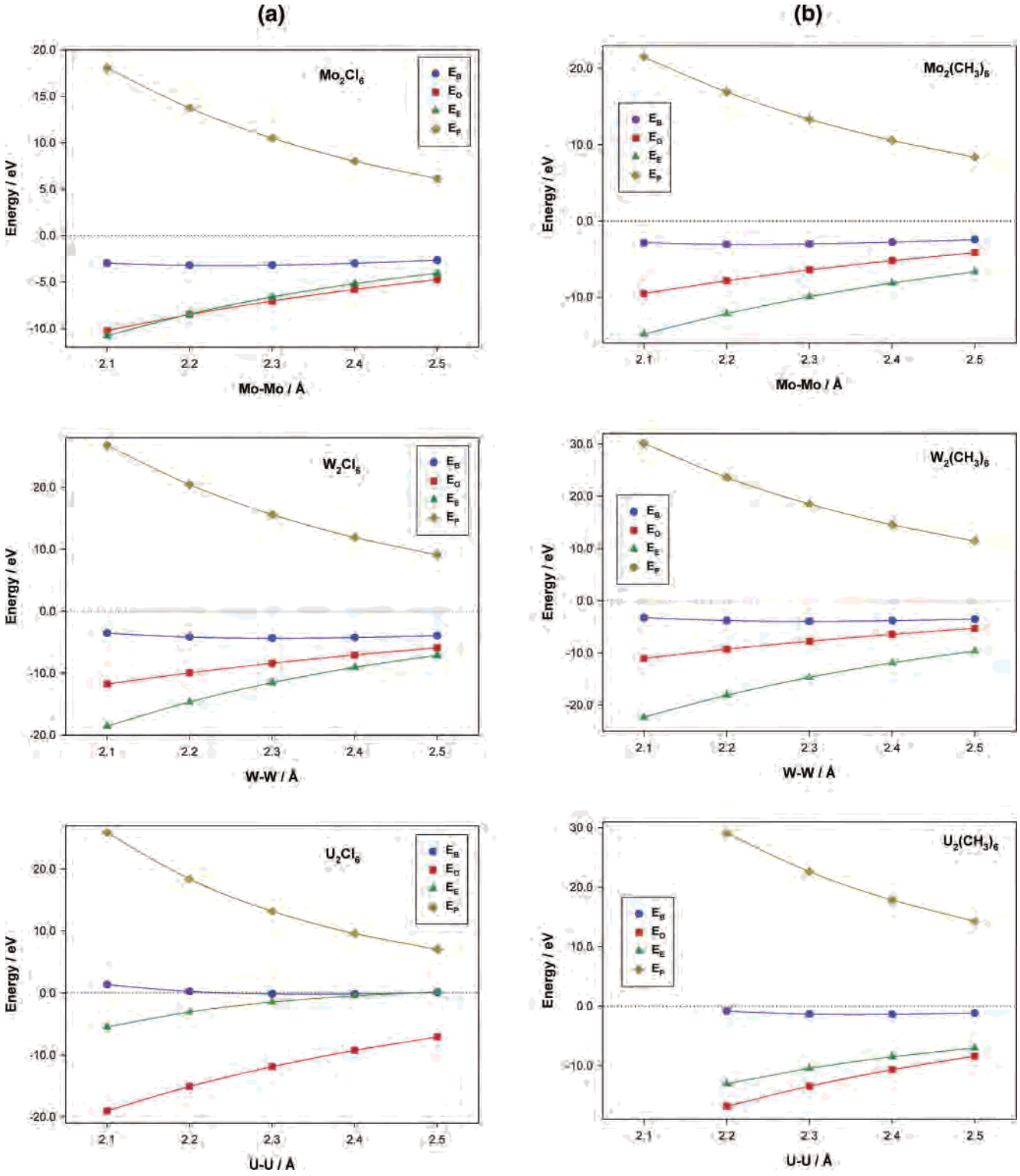

Figure 3. Potential energy curves for (a) M_2Cl_6 and (b) $M_2(CH_3)_6$ complexes in the 210−250 pm range of metal−metal distances.

ment orbital overlaps,[30] and that the electron density distribution along bond axes should be taken into account for the interpretation of electrostatic interaction results.[31]

At the equilibrium metal−metal distances, the overlaps between occupied fragment orbitals in the Mo, W, and U complexes investigated have similar values, correlating with the fact that the Pauli repulsion across the three series is of comparable magnitude (as noted in the preceding section). The fully occupied orbitals of the MX_3 fragments are predominantly ligand-based, with the relatively small metal contributions having primarily d character in the Mo and W species and a combination of d and f character in the U species (see Section 3.1). These general similarities in the

(30) Bickelhaupt, F. M.; Bickelhaupt, F. *Chem. Eur.*−*J.* **1999**, *5*, 162.
(31) Lein, M.; Szabó, A.; Kovács, A.; Frenking, G. *Faraday. Discuss.* **2003**, *124*, 365.

Table 6. Energy Decomposition Analysis of M_2Cl_6 and $M_2(CH_3)_6$ Complexes Calculated at a Fixed Metal−Metal Distance of 230 pm[a]

		Energy Decomposition Result (eV)				
ligand	metal	E_B	$E_P + E_E$	E_P	E_E	E_O
Cl	Mo	−3.19	3.86	10.47	−6.61	−7.05
Cl	W	−4.36	4.05	15.58	−11.53	−8.41
Cl	U	−0.16	11.72	13.19	−1.47	−11.89
CH_3	Mo	−3.02	3.39	13.34	−9.95	−6.41
CH_3	W	−3.97	3.80	18.50	−14.70	−7.77
CH_3	U	−1.34	12.13	22.60	−10.47	−13.46

[a] Results correspond to eq 3. Legend for table is as follows: E_B, total bonding energy; E_P, Pauli repulsion, E_E, electrostatic interaction; and E_O, orbital mixing.

Table 7. Comparison of Energy Decomposition Analyses of Mo and U Complexes, Using Basis Sets with Large (Mo.4p, U.6p) and Small (Mo.3d, U.5d) Cores[a] (Results are Given as the Difference, δE, between the "Large-Core" and "Small-Core" Calculation)

		Difference (eV)			
metal	ligand[b]	δE_B	δE_P	δE_E	δE_O
Mo	Cl	−0.11	−0.53	0.24	0.13
Mo	F	−0.07	−0.35	0.16	0.14
Mo	OH	−0.14	−0.37	0.08	0.15
Mo	NH_2	−0.28	−0.47	0.12	0.08
Mo	CH_3	−0.33	−0.41	0.07	0.00
U	Cl	−5.04	−6.29	0.03	1.22
U	F	−4.29	−6.11	0.42	1.39
U	OH	−4.45	−5.68	0.40	0.83
U	NH_2	−4.91	−5.63	−0.24	0.95
U	CH_3	−6.21	−7.40	1.10	0.11

[a] Results correspond to eq 3. Legend for table is as follows: E_B, total bonding energy; E_P, Pauli repulsion, E_E, electrostatic interaction; and E_O, orbital mixing. [b] The results may be less accurate for $U_2(CH_3)_6$ than for the other complexes, because of rather severe convergence difficulties that were encountered in the calculations on the $U(CH_3)_3$ fragments.

fragment orbital compositions may also contribute to the comparable results obtained for the three series of complexes.

The magnitude of the Pauli term varies across each individual series, and more noticeably for the U complexes than for the Mo and W analogues, but a common result is observed in the fact that the $M_2(CH_3)_6$ species exhibit the highest values for each metal. This result correlates with the relatively greater metal character found in the occupied $M(CH_3)_3$ orbitals, which translates into more significant overlap between the fragment orbitals and stronger Pauli repulsions.

We have mentioned that, at the respective optimized metal−metal distances, the electrostatic interaction is weaker in the U species, relative to the Mo and W complexes, and that, in some cases, this is partly due to the longer equilibrium bond lengths. Another factor, which may have a more general influence and play a more significant role, is observed in the comparison of the nature and properties of the $6a_1$ fragment orbitals (Figure 4).

These orbitals are largely metal-based, and the major contributions come from functions of d_{z^2} and f_x character for d-block and U complexes, respectively, with significant s character also being predicted. The plots in Figure 4 show that the d(s)-type $6a_1$ orbital of the WCl_3 fragment lies along the W−W axis and extends significantly toward the opposite metal site, whereas the f(s)-type $6a_1$ orbital of the UCl_3 fragment is more evenly spread along the directions parallel and perpendicular to the U−U axis and does not reach as far toward the opposite metal site. This greater radial extension of the fragment orbitals in the W species, relative to the U systems, should result in more significant overlap between the electron density on a given fragment and the metal atom nucleus in the opposite fragment, and thus lead to stronger attractive electrostatic interactions. The results for the Mo complexes are similar to those observed for the W species, but the Mo-based orbitals are generally more contracted, which is consistent with the smaller values obtained for the bonding energy components.

Although the electrostatic interactions are generally weaker in the U complexes, relative to the W and Mo analogues, the calculated values are particularly small for U_2Cl_6 and U_2F_6. A possible explanation may lie in the somewhat less significant contributions of U s-type functions to the composition and character of the corresponding fragment orbitals.

3.2.3. Post-relaxation: Orbital Mixing Interactions. We noted in Section 3.2.1 that, although the overall metal−metal interactions are weaker in the U complexes, relative to the W and Mo analogues, the opposite result is observed for the orbital-mixing component. Further insight can be gained by decomposing the orbital interactions in terms of C_{3v} irreducible representations, as shown in Table 5.

In C_{3v} symmetry, the major contributions to the orbital interactions between the MX_3 fragments are associated with the a_1 and e representations, which correspond to metal−metal σ and π bonding, respectively. The calculated values of the a_2 component are not strictly zero, but are nonetheless negligibly small, because there are no directly relevant orbital interactions between the metal atoms that transform as this irreducible representation.

The larger magnitude of the orbital mixing term in the U complexes arises from stronger interactions of both σ and π types, with the difference between the relative a_1 and e contributions, in the U systems, with respect to the W or Mo species, being more significant for the e component. A general rationale for these results may be observed in the fact that the orbitals required for metal−metal σ and π bonding are more extensively involved in metal−ligand bonding in the Mo and W complexes than the U analogues and, consequently, the participation of these orbitals in metal−metal bonding is greater in the U species, compared to the W and Mo systems.

In the Mo and W complexes, metal−metal σ and π bonding primarily results from interactions between, respectively, d_{z^2} and d_{xz} or d_{yz} orbitals that also exhibit relatively significant participation in metal−ligand interactions. The nature of the metal−metal and metal−ligand interactions is somewhat different in the U complexes, as bonding between the U atoms is realized predominantly through f_{z^3} (σ-like) and f_{z^2x} or f_{z^2y} (π-like) orbitals that are not strongly involved in bonding to the ligands, partially due to the fact that the metal−ligand interactions in the U complexes have mixed U d and f character.

The average percentage contributions of the a_1 and e components to the total orbital mixing energy are 42:58,

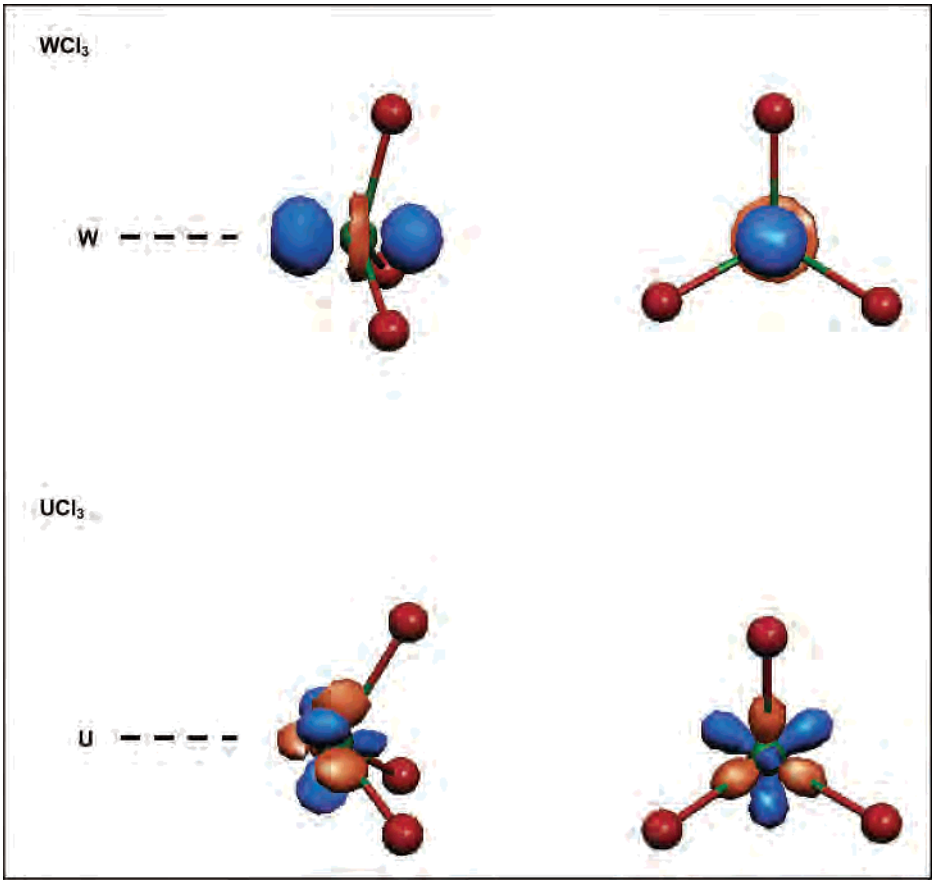

Figure 4. Spatial representation of the $6a_1$ orbital in WCl_3 and UCl_3 fragments, viewed both perpendicular to and along the C_3 rotational axis.

41:59, and 37:63 (a_1:e) for the Mo, W, and U species, respectively. The participation of the Mo and W d_{xz} or d_{yz} orbitals in the metal−ligand interactions is more significant than that of the d_{z^2} orbitals, and this may be the reason for the greater difference in the relative magnitudes of the e (π) components, with respect to a_1 (σ) components, between the U and W or Mo complexes.

Table 5 shows that, in the Mo and W series, the $M_2(NH_2)_6$ complexes exhibit the lowest bonding energy, and this result can be traced to the reduced strength of the metal−metal π-like interactions. The molecular orbital analysis suggests that the relative weakness of metal−metal π bonding in these species may be a consequence of a comparatively stronger involvement of the metal d_{xz} and d_{yz} orbitals in the interactions with the ligands.

Table 5 also reveals that the highest bonding energy in the U series is for the $U_2(CH_3)_6$ species, largely due to strong a_1 (σ) and e (π) orbital mixing contributions. The π-like component of U−U bonding in $U_2(CH_3)_6$ is predicted to be particularly strong, and this can be attributed to the fact that, in addition to the primary π-like interaction associated with the $6e_u$ orbitals of predominantly f_{z^2x} or f_{z^2y} character, there is a second rather significant U−U interaction, which corresponds to the $5e_u$ level and involves the U d_{xz} and d_{yz} orbitals.

We have shown in Section 3.2.2 that a comparison of the nature and properties of the $6a_1$ fragment orbitals can be used to rationalize the predicted differences in the magnitude of the electrostatic interaction, which is generally greater for the Mo and W complexes than for the U analogues. However, the opposite result holds for the a_1 (σ) component of the orbital mixing energy, and a possible explanation can be found in Figure 2. In the Mo and W complexes, metal−metal σ bonding is largely dominated by interactions between the $6a_1$ fragment orbitals, whereas both the $6a_1$ and $7a_1$ orbitals of the UX_3 fragments are important in U−U σ bonding. The $7a_1$ orbitals have a particularly significant role, by providing the predominantly f_{z^3} character of the $6a_{1g}$ orbitals in the U complexes.

4. Conclusions

The molecular and electronic structures of a series of U, W, and Mo M_2X_6 complexes have been investigated by relativistic density functional methods, and a detailed analysis of the metal−metal interactions has been performed using molecular orbital theory and energy decomposition approaches.

Multiple bonds between the metal atoms are observed for all species investigated. The orbital properties of these metal−metal bonds can be described as a combination of σ and π interactions, with predominant d−d character in the Mo and W complexes and f−f character in the U systems. The overall metal−metal bond strength is predicted to be substantially greater in the Mo and W species, with respect to the U analogues. The relative weakness of U−U bond is a consequence of the significantly more destabilizing nature

of the "pre-relaxation" Pauli-plus-electrostatic effects in the interaction between the MX_3 fragments, suggesting that there are intrinsic intramolecular reasons why metal−metal bonding is so scarce in the 5f block. However, the "post-relaxation" fragment interactions, associated with orbital mixing effects, are stronger in the U complexes.

The greater strength of the metal−metal orbital interactions in U_2X_6, with respect to W_2X_6 and Mo_2X_6 species, shows a correlation with the nature and properties of the metal−ligand bonds. In the Mo and W complexes, metal−ligand bonding exhibits a higher degree of covalency than in the U systems. Furthermore, the Mo and W d orbitals involved in metal−metal bonding, particularly π-like bonding, also participate, to a significant extent, in the interactions with the ligands. In contrast, the f orbitals primarily responsible for U−U σ and π bonding have a comparatively less important role in the metal−ligand interactions, which have a combined U f and d character, but with the latter, predicted to be somewhat more significant. This situation is reminiscent of Bursten's description[9] of the electronic structure of (early) actinide complexes, in terms of the "dichotomy of roles served by the 6d and 5f orbitals", which are primarily used to bind ligands or to accommodate metal-based electrons, respectively. In the present U_2X_6 species, although the metal−ligand interactions do exhibit some U 5f character, the U f_{z^3} (σ-like) and f_{z^2x} or f_{z^2y} (π-like) orbitals remain largely unaffected and are, thus, available for the formation of the U−U ($\sigma + 2\pi$) triple bond.

Pauli repulsion effects are observed to be of comparable magnitude across the three series of M_2X_6 complexes, and, therefore, the electrostatic interactions seem to be the primary reason for the relative overall weakness of the U−U bonds, compared to the W−W and Mo−Mo bonds. For some U species, most notably U_2Cl_6, the electrostatic component of the bonding energy is extremely small, but even for species such as $U_2(OH)_6$ and $U_2(CH_3)_6$, where the electrostatic effects are rather stronger, the relative stabilization provided is not sufficient to counteract the destabilizing Pauli repulsion to a degree comparable to that observed for the Mo and W complexes. A possible explanation for the relatively weak electrostatic interactions in the U_2X_6 species lies in the fact that the U−U equilibrium bond lengths are somewhat longer (than the optimized W−W and Mo−Mo distances) and some properties of the relevant fragment orbitals (extension and directionality) may not be as favorable as in the W_2X_6 and Mo_2X_6 species. These two factors lead to less significant overlap between the electron densities and metal nuclei on opposite fragments, thus resulting in reduced stabilization from the Coulombic attractions.

Acknowledgment. We are grateful for financial support from the Engineering and Physical Sciences Research Council (under Grant No. EP/C533054) and for the allocation of supercomputer time from the National Service for Computational Chemistry Software. We are also grateful to the reviewers for their helpful comments.

Supporting Information Available: Tables S1 and S2 describe tests of functional performance in the calculation of metal−metal distances in Mo and W $M_2(NH_2)_6$ and $M_2(CH_3)_6$ and U_2Cl_6 complexes, and Tables S3, S4, and S5 contain data from extended energy decomposition analyses (along the potential energy curves) of all species investigated. (PDF file.) This material is available free of charge via the Internet at http://pubs.acs.org.

IC060777E